Journal of Engineering and Development, Vol. 11, No. 2, September (2007) ISSN 1813-7822

Simulation of Satellite Telemetry-Telecommand Coherent Transponder

Asst. Prof. Dr. Adil Hameed Ahmad
Electrical Engineering Department
University of Technology, Baghdad, Iraq

Eng. Samer Majid Mohsen
Satellites Technology Center
Ministry of Science & Technology, Baghdad, Iraq

Abstract

The Telemetry/Telecommand Transponder is the unit on board a satellite that maintains the communication link between the satellite and the control center on the Earth. The spacecraft includes service telecommunications Telemetry and Telecommand (TMTC) and On-Board Supervision (OBS) subsystem to provide telemetry, telecommand and ranging functions during all phases of the mission.

The function of transponder, generally, is receiving the uplink signal modulated with telecommand and ranging tones, process it, and transmit the downlink signal (at different frequency) modulated with telemetry and ranging signal to the ground station. In this research, European Space Agency's recommendations and standard have followed to calculate the coherent transponder parameters.

The coherent transponder and the related communication functions have been simulated using MATLAB Simulink software version 6.5. The computer simulation was necessary to show the performance of such functional block under the influence of many parameters like Doppler shift, input signal level variation, and damping factor variation.

الخلاصـــــة

المرسل المستجيب لاستلام الاوامر وارسال البيانات هو جزء من منظومة القمر الصناعي والذي يحافظ على وجود قناة الاتصال بين القمر الصناعي ومركز السيطرة الارضية. ان المركبة الفضائية تتضمن خدمات اتصالات بعيدة (استلام الاوامر وارسال البيانات) ومنظومة الاشراف السطحي وذلك من اجل توفير البيانات والاوامر ووظائف قياس المدى خلال كل اطوار الرحلة الفضائية .

وظيفة المرسل المستجيب،عموما، هو استلام الاشارة الصاعدة والمضمنة ببيانات الاوامر واشارة المدى ومعالجتها وبث الاشارة النازلة وبتردد مختلف ومضمن فيها بيانات عمل منظومة القمر الصناعي واشارة المدى الى المحطة الارضية. في هذا البحث، توصيات ومعايير وكالة الفضاء الاوربية تم اتباعها لحساب متغيرات المرسل المستجيب المتشاكه.

ان المرسل المستجيب المتشاكه ووظائف الاتصالات المتعلقة به قد تم تمثيلها باستخدام برنامج MATLAB SIMULINK ذو الاصدار 6.5 . المحاكاة الحاسوبية كانت ضرورية لاظهار اداء الاجزاء الوظيفية تحت تأثير تغيير عدة متغيرات مثل زحزحة الدوبلر، تغيير مستوى اشارة الادخال وتغيير معامل التخميد.

1. Introduction

Telemetry, Tracking and Command are vital functions of a spacecraft. They allow data to be communicated between the ground and the spacecraft for spacecraft control and command. TTC transponder on the spacecraft plays the role of Radio Frequency (RF) interface with the ground [1]. TTC's functions can be divided into three major parts:

1. **Telecommand link:** which is used to upload commands to the spacecraft. Telecommanding is of particular importance to deep-space probes. Their distance from the earth creates communication problems. Firstly, the signals reaching the probe from the ground are so weak that the amount of data that can be transmitted is limited. Secondly, it can take up several hours for the radio signal from earth to reach the probe if the probe is at the edge of the solar system, which makes controlling the probe extremely difficult [2].

2. **Telemetry link:** which is equally important to the success of a satellite mission. Telemetry is the data received from the spacecraft, generally about the status of its systems. Throughout the mission, it enables the mission control center to survey the "insides" of the spacecraft, its configuration, its status, and in the case of failure, it provides the basis for the decisions that have to be made [2,3].

3. **Tracking and Ranging link:** The transponder demodulates the ranging signal contained in the uplink and remodulates it onto the downlink. Moreover, the transponder has the ability to generate a downlink carrier phase coherent with the uplink carrier, allowing precise estimations of orbit and speed from measurements of Doppler offset and rate of the downlink frequency at the ground station [3]. The architecture of a typical spacecraft TTC system is shown in **Fig.(1)**.

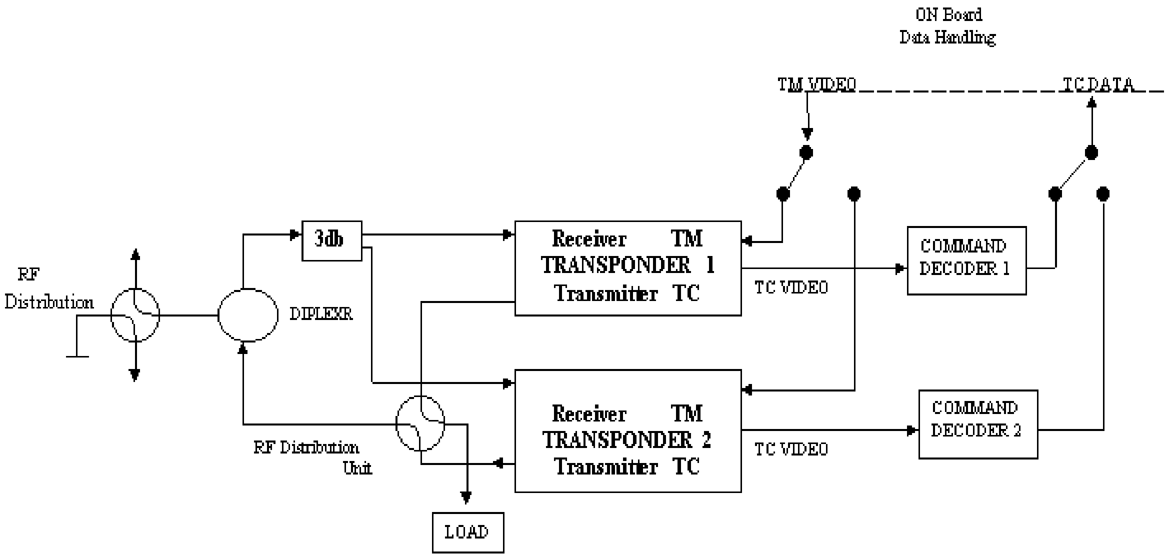

Figure (1) Architecture of a typical spacecraft TTC system

The internal architecture of a TTC transponder is shown in **Fig.(2)** [2].

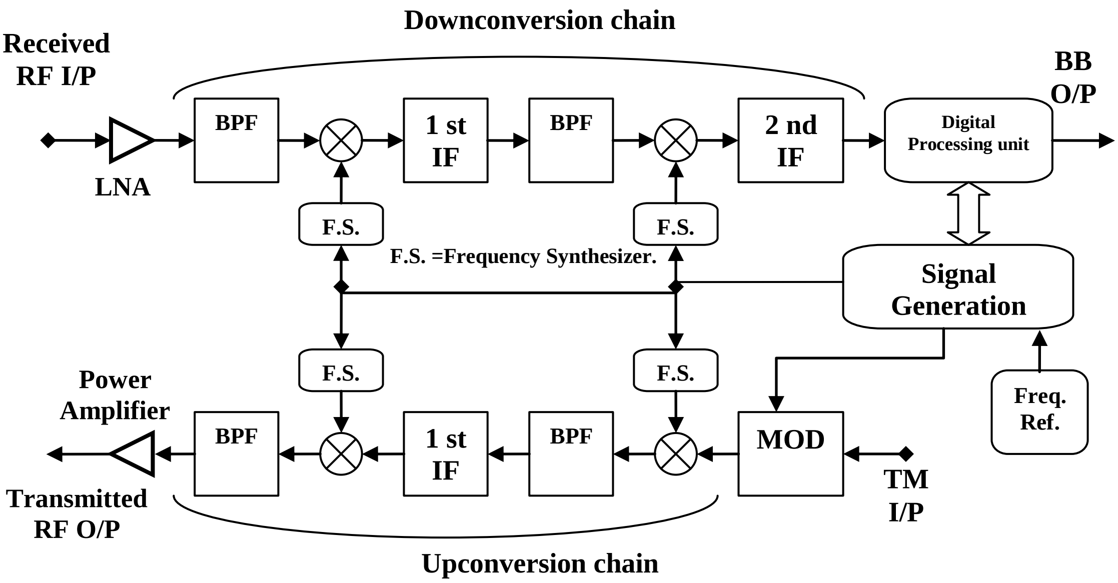

Figure (2) Block diagram of a typical TTC transponder

In practice, with respect to TTC transponders, there are three different types of space applications:

A) Deep Space Missions (DS):

To improve reception, coherency between up and down links via fixed turn-around ratios is normally utilized. Dual frequency downlinks (S and X band simultaneously) are also used to counter ionospheric delay and achieve better orbit determination accuracy [4].

B) Near Earth Missions (NE):

Generally, the absolute power is not a concern in these missions, but some of them have a highly eccentric orbit which for the transponder, means that the signals received from the ground station when the satellite is at apogee have a low level while the signal that the transponder receives when the satellite is at perigee is proportionately considerably higher. The transponder, therefore, has to be able to cope with a dynamic range in the received signal that can be as high as 70 dB [5].

C) Low Earth Orbit (LEO) and Transmission via Data Relay Satellites (DRS):

The third class of application is satellites in LEO that transmit their TTC signals either directly to ground or via a DRS. Data relay satellites are not free to radiate a large amount of power at earth's surface because it might cause interference to terrestrial users [4,5].

National Aeronautics and Space Administration (NASA) first implemented a coherent transponder in the sixties of the last century by applying phase lock techniques. Until 1980, the technology used in the transponders was primarily analogue. From 1990 to 2000, progress has been made in miniaturization (MMIC and ASIC), and digitization of the demodulation, modulation and frequency generation functions [4]. As an example, the Automated Transfer Vehicle (ATV) proximity link transponders are oriented to have reliable links with the International Space Station (ISS). One is implemented in the ATV and the other one is implemented with particular constrains in the ISS [6]. Also, as part of ESA's living planet programme, the Gravity Field and Steady State Ocean Circulation Explorer (GOCE) satellite will be in orbit for a minimum of two years to provide data about solid earth physics, ice sheet dynamic and sea level changes. The GOCE spacecraft is scheduled for launch in 2005. As a new feature, this transponder will work with both PM and QPSK modulations selectable by telecommand. Thus, it will be possible to configure the transmitter either for ranging measurement or for high data rate transmission [7].

2. Telemetry/Telecommand System Configuration

The Telemetry/Telecommand (TMTC) subsystem represents the interface between the spacecraft onboard subsystem and the TTC ground station. This subsystem performs multiple functions [8]:

a) Telemetry: the telemetry function is the acquisition, encoding, and transmission to ground of the data necessary to control the satellite and establish the performance of all on-board subsystems.

b) Telecommand: the telecommand function is the reception, decoding and distribution of coded messages sent from the ground station to control or change the operational status of the satellite.

c) Ranging: the ranging function is the relaying of ranging encoded tone sent by the ground TTC station, enabling the ground station to perform range and range-rate measurements.

2-1 Ground Segment TTC Operation

Down link signal received by the antenna fed through duplexer to receiver part. After appropriate low noise amplification and down conversion the signal are distributed to, Telemetry, Ranging and Tracking units. Azimuth and elevation errors are fed to the servo system to steer the antenna to the signal source. From receivers the signal is down converted to suitable IF band and applied to the IF combiner for combination of signals with any polarization. After combiner, IF signals distributed to demodulators and to the tracking subsystem. A simplified purpose ground station is shown in **Fig.(3-a)** [1, 4].

2-2 Space Segment TTC Operation

The typical architecture of a satellite TTC subsystem is shown in **Fig.(3-b)** [1].

The uplink carrier with telecommand (TC) signal from the ground station is received by the TTC antenna and applied to receiver input via the diplexer. The signal consists of a radio frequency carrier, phase-modulated subcarrier itself BPSK modulated by TC data. The receiver outputs the modulate subcarrier at base band to the active decoder. The decoder recovers the TC data and sends it to the On-Board Data Handling "OBDH" [2].

Generally, the function of transponder is to receive radio frequency signal modulated with telecommand and ranging information from the TTC ground station, process it, and transmits RF signals (at different frequency) modulated with the telemetry and ranging information to the TTC station. The coherent transponder performs the communications and range measurement by phase locking the RF carrier of the downlink to that of the up link [8].

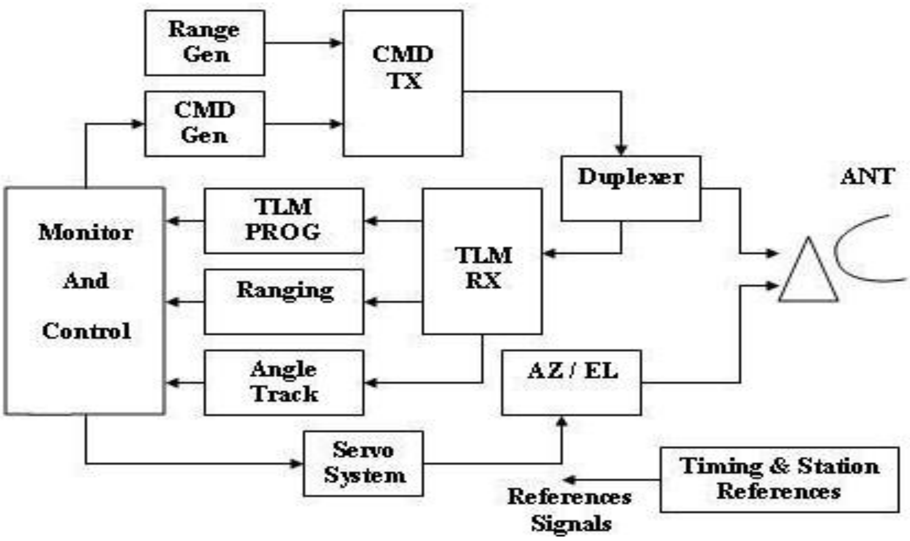

Figure (3-a) Simplified block diagram of TTC ground station

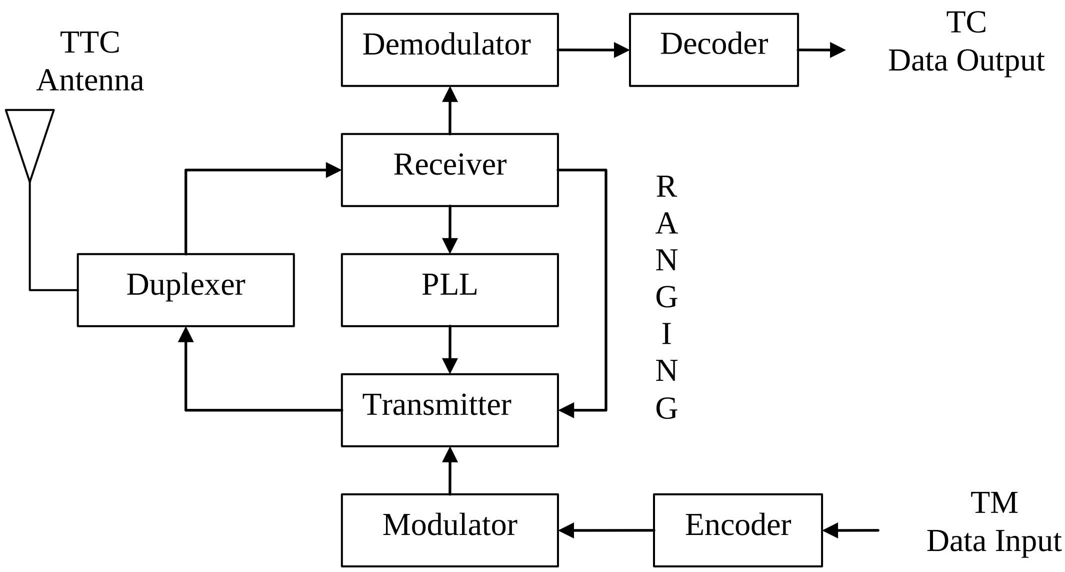

Figure (3-b) Satellite TMTC subsystem block diagram

2-3 TMTC Operating Modes and Modulation Limitations

Different operating modes are possible for TMTC functions. The following operating modes are possible [9]:

Mode	Uplink	Downlink
1	Telecommand (TC)	....
2	....	Telemetry (TM)
3	Ranging (RNG)	Ranging + Telemetry (RNG + TM)
4	Telecommand (TC)	Telemetry (TM)
5	Ranging + Telecommand (RNG + TC)	Ranging + Telemetry (RNG + TM)

ESA standard gives details of the modulation limitations [1,9]. These limitations are shown in **Tables (1)** and **(2)** for both telecommand and telemetry.

Table (1) PCM waveform and rate

RF Carrier (MHz)	Function	Symbol rate (Hz)	PCM waveform
2025- 2120	Telecommand	$4000 / 2^n$ n=1, 2,…….9.	NRZ-L
2200 – 2300	Telemetry	$10^2 – 10^6$	NRZ-L

Table (2) Subcarrier used with phase-modulated RF carrier

RF Carrier (MHz)	Function	Subcarrier (KHz)	Modulation waveform	Subcarrier waveform
2025-2120	Telecommand	8 or 16	NRZ –L	Sine
2200-2300	Telemetry	0.1 - 100	NRZ-L	Sine

2-4 TMTC Requirements and Parameters Calculation

The transponder consists of a receiver (RX) chain including Low Noise Amplifier (LNA), one or more down conversion mixers, intermediate frequency (IF) amplifiers, automatic gain control (AGC), a telecommand demodulator (TC Demodulator), and a transmitter (TX) chain including a telemetry modulator (TM Modulator) and a power amplifier. The required frequencies are synthesized from a Voltage Controlled-Crystal Oscillator (VCXO) reference. A duplex filter separates the RX and TX frequencies [10]. The first step of the spacecraft transponder design begins with choosing the input and output frequencies at which the transponder will operate. It is required to calculate the PLL loop parameters based on the given information about Doppler frequency shift, loop filter bandwidth and damping factor. The next step starts with achieving the requirements and design of TC demodulator, Ranging detection and TM modulator.

2-5 Design Review of Phase-Locked Transponder

For Doppler measurement to have any meaning, the return signal must be coherent (both in phase and frequency) with the uplink signal [11,12]. A block diagram of a typical phase locked transponder is shown in **Fig.(4)**.

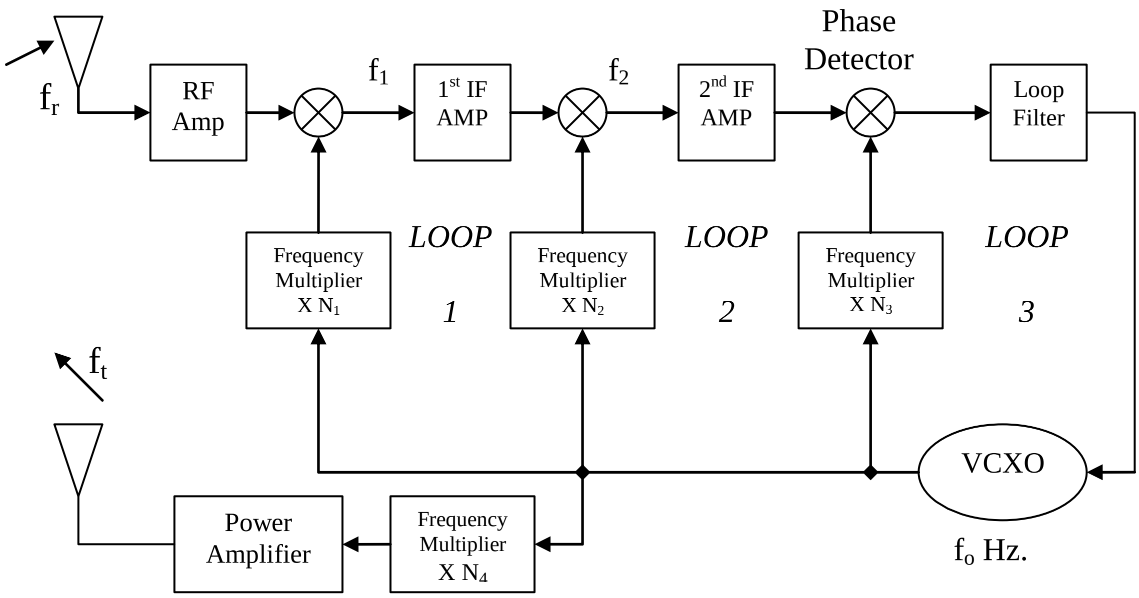

Figure (4) Phase locked transponder

Operation of the first mixer may be described by:

$$\mathbf{f_r = N_1 f_o \pm f_1} \quad \text{.......} \quad \mathbf{(1)}$$

While the operation of the second mixer may be given by:

$$\mathbf{f_1 = N_2 f_o \pm f_2} \quad \text{.......} \quad \mathbf{(2)}$$

And the phase lock requirement, is

$$\mathbf{f_2 = N_3 f_o} \quad \text{.......} \quad \mathbf{(3)}$$

A combination of these three equations and elimination of the two intermediate frequencies result in,

$$\mathbf{f_r = f_o (N_1 \pm N_2 \pm N_3)} \quad \text{.......} \quad \mathbf{(4)}$$

Because the transmitted frequency is

$$\mathbf{f_t = N_4 f_o} \quad \text{......} \quad (5)$$

The ratio of output frequency to input is

$$\frac{f_t}{f_r} = \frac{N_4}{N_1 \pm N_2 \pm N_3} \quad \text{......} \quad (6)$$

where:

f_r: is the transponder received frequency (from TTC ground station);

f_t: is the transponder transmitted frequency (to TTC ground station);

N_1, N_2, N_3 and N_4: are the frequencies multiplying factors.

From equation (6), the Space-to-Earth link carrier frequency shall be derived coherently from the Earth-to-Space link carrier frequency. Thus, the transponder is coherent if it is locked.

The active loop filter requires a high gain DC amplifier, but provides better tracking performance [11,12,13]. The parameters related to PLL can be expressed as:

$$\omega_n = \left(\frac{K_{PD}K_{VCO}}{\tau_1}\right)^{1/2} \quad \text{......} \quad (7)$$

$$\eta = \omega_n \frac{\tau_2}{2} \quad \text{......} \quad (8)$$

where:

K_{PD}: is the phase detector gain factor measured in volts per radian;

K_{VCO}: is the VCO constant measured in radian per second per volt;

ω_n: is the natural frequency of the loop;

η: is the damping factor.

The 3 dB bandwidth is given by [12,13]:

$$\omega_{3dB} = \omega_n \left[2\eta^2 + 1 + \sqrt{(2\eta^2 + 1)^2 + 1}\,\right]^{1/2} \quad \text{......} \quad (9)$$

3. Transponder Design

For S-band, the coherent mode ratio of the output frequency f_t to the input frequency f_r is selected according to the ESA standard which uses the ratio (f_t/ f_r) of (240 / 221) [10, 12]. A possible way to achieve this is by selecting $N_1 = 108$, $N_2 = 3$, $N_3=0.5$ and $N_4 = 120$ [12].

Refer to the basic block diagram of the coherent transponder, which is shown in **Fig.(4)**, it is shown that the ratio of the output frequency "f_t" to the input frequency "f_r" is $\frac{f_t}{f_r} = \frac{N_4}{N_1 + N_2 - N_3}$

3-1 Phase Locked Loop Requirements

The phase locked loop requirements are set as follows:

I) VCO Free–Running Frequency (f_o): This frequency corresponds to the received and transmitted frequencies of the transponder when no Doppler shift exists. For f_t = 2250 MHz and N_4 = 120. Then, $f_o = \frac{2250MHz}{120}$ = 18.75 MHz. As a design parameter, it is clear that a VCO frequency of 18.75 MHz is chosen which results in f_t = 2250 MHz and f_r = 2071.875 MHz. These frequencies (f_t and f_r) lie almost in the center of the ESA frequency band.

II) PLL Lock–Range (± Δf): This corresponds to the frequency range of the PLL circuit where the PLL stay in lock with f_{If2} when the received frequency is changing due to Doppler shift f_d with maximum value of ± 60 KHz [9]. For locked condition, with Doppler shift ($f_o + \Delta f$) $= \frac{f_r + f_d}{N_1 + N_2 - N_3}$. For N_1 = 108, N_2 = 3, N_3 = 0.5 and f_d = ± 60 KHz therefore, Δf = ± 0.543 KHz. So the required PLL lock range = 1.086 KHz.

III) PLL Filter Bandwidth: $2B_L = 800\ Hz$ [1, 9].

IV) Damping Factor: η is chosen between (0.707 – 1) for maximally flat response [1,14,15].

3-2 TMTC Subsystem Design

The subsystem design starts with putting a functional block diagram of a Coherent Transponder that satisfies ESA standards. The functional TMTC transponder system can be divided into individual TMTC subsystems. **Figure (5)** shows the TMTC Transponder functional block diagram.

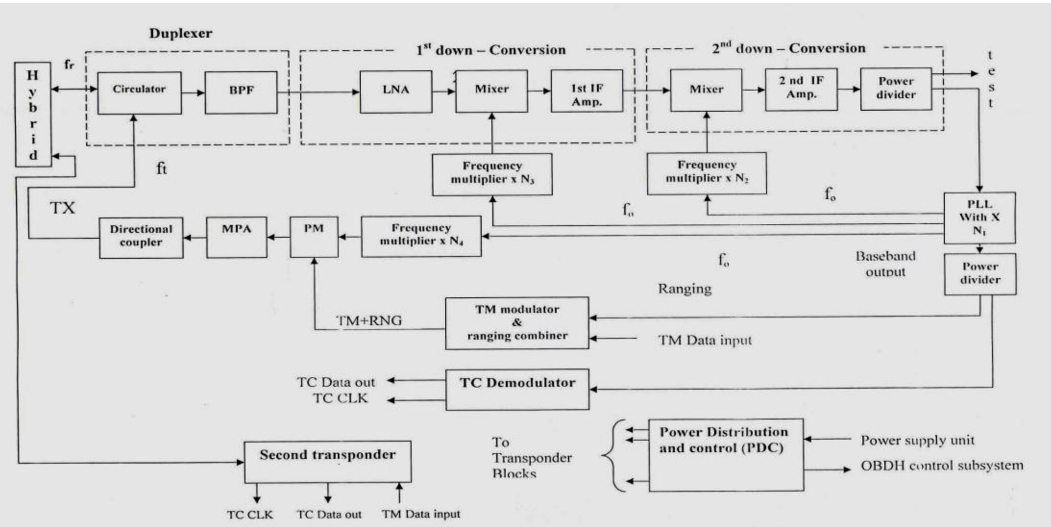

Figure (5) TMTC Transponder functional block diagram

The following subsections describe the design of PLL unit and TC demodulation

3-2-1 Phase Locked Loop Design

It is shown in the literature that the order of a PLL system is decided by the nature of the input signal that it has to lock and track [13]. A modified second loop with perfect integrator can provide a constant tracking phase error with input frequency velocity signal [14]. The following steps show the calculation of the PLL loop parameters:

1. The VCO block at 18.75 MHz has frequency sensitivity constant K_{VCO} =1 KHz/V while the sensitivity of the phase detector K_{PD} is 0.458 V/rad. The loop gain is given as:

$K = K_{PD}\, K_{VCO}\, N$ where N = frequency multiplication factor. Therefore,

$$K = (0.458\frac{v}{rad}) * (2\pi * 1000\frac{rad/\sec}{v}) * 110.5 = 317.986 * 10^3 \sec^{-1}.$$

2. The natural loop frequency ω_n can be calculated since the PLL loop bandwidth is given and the value of the damping factor is selected based on ESA standards as η = 0.8. Since $2B_L$ = 800 Hz. (given), then; B_L = 400 Hz. Therefore,

$$400 = \frac{\omega_n}{2\pi}\left[2(0.8)^2 + 1 + \sqrt{2(0.8)^2 + 1 + 1}\right]^{1/2}$$, solving for ω_n gives, ω_n = 1150rad/sec.

3. Filter's time constant τ_2 can be computed as follows:

$0.8 = 1150\frac{\tau_2}{2}$, solving to get, $\tau_2 \approx 1.4$ msec.

4. Filter's time constant τ_1 can be determined as shown:

$$\tau_1 = \frac{317.986\times10^3}{(1150)^2} = 240 \text{ m sec.}$$

With the above-calculated parameters, the overall performance of a basic PLL will be examined under the influence of different factors in such away to show the relationship of the PLL parameters upon both the error signal and the VCO input/output signal.

3-2-2 TC Demodulator

The main function of the Telecommand demodulator is to extract the telecommand data from the BPSK signal coming from the PLL unit. The other function of such unit is to generate timing reference signal for NRZ digital data also to provide lock indication facility, which is to be sent back to the ground control station as telemetric data. Reinsertion of the carrier can be performed by a variation of a standard PLL called a Costas loop [15]. A typical block diagram of the Costas carrier recovery loop is shown in **Fig.(6)**.

It is clear that the loop can lock with the VCO at two different angles relative to the phase of the input signal, i.e, when $\sin 2(\theta_i - \theta_o)$ is zero for 0º and 180º. For small phase error, $\sin 2(\theta_i - \theta_o)$ can be approximated to $2(\theta_i - \theta_o)$. Thus the equivalent gain of the phase detector,

K_{PD}, will be: $K_{PD} = \frac{1}{8} K_m (A_i\, A_o)^2$ **……………………………………….. (11)**

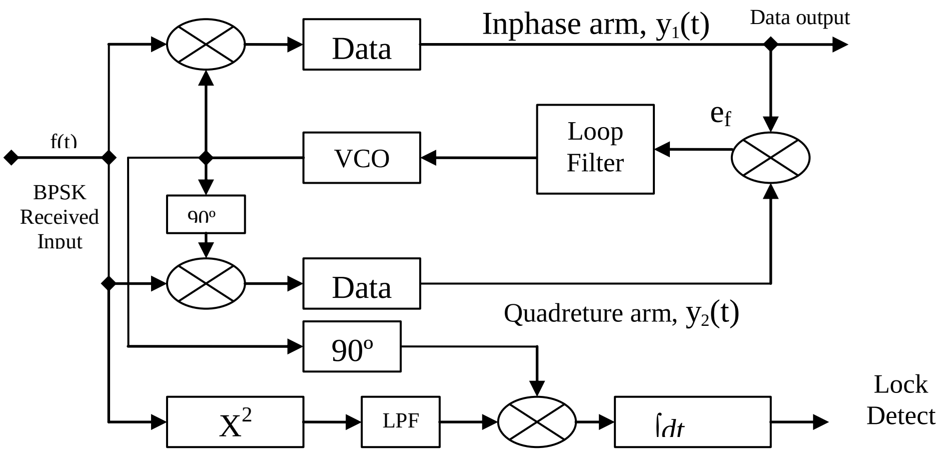

Figure (6) Typical PSK demodualtion

The equivalent PLL block diagram for a Costas loop is shown in **Fig.(7)**.

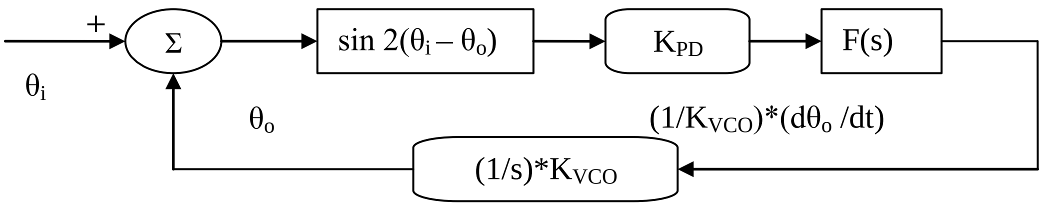

Figure (7) Equivalent PLL block diagram for a costas loop

The received 8 KHz BPSK Telecommand signal, which is modulated by 2kbps binary data, could be carrier synchronized in ten-bit periods. The input received signal level is unity as well as the VCO reference level. Based on the above requirements, we can calculate the parameters as follows:

- t = time of acquisition = 10 * bit period = $10 * \left(\frac{1}{2000}\right)$ = 5 m sec.
- The loop settles to within 5% for ω_n = 900 rad/sec. Also for $\omega_n t = 4.5$, the damping factor of $\eta = 0.8$ is the optimum value as shown in figure (8).
- loop filter time constant $\tau_2 = \left(\frac{2*0.8}{900}\right)$ = 1.77 m sec.
- Choosing a VCO with sensitivity of K_{VCO} = 1000 Hz/V, phase detector constant will be $K_{PD}=0.125 * K_m$. Select $K_m = 50$, then $\tau_1 = \left(\frac{0.125*50*6280}{900^2}\right)$ = 48.45 m sec.

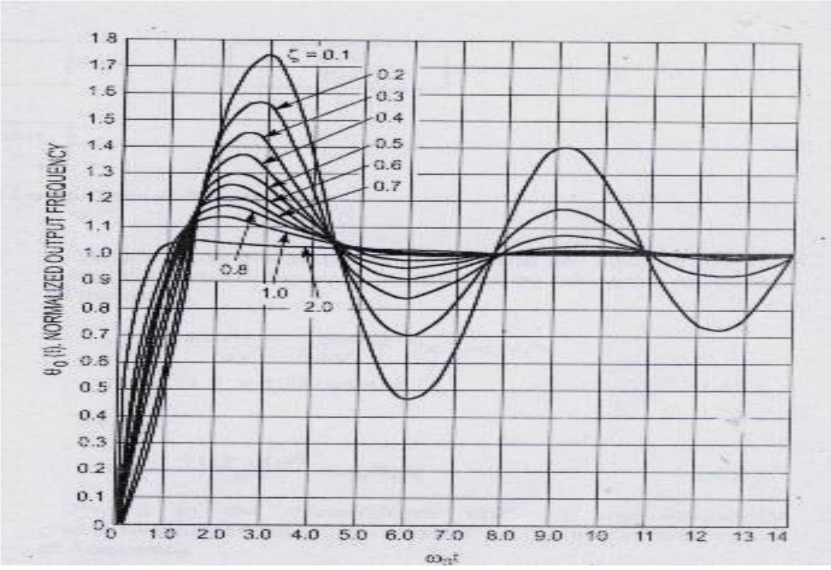

Figure (8) Second order step response

4. Computer Simulation and Results

The simulation has been performed using MATLAB simulink version 6.5. In this paper, the main loop (Loop 3) of the coherent transponder was simulated and tested first. The simulation is concerned with many items such as: characteristics of phase detector, error signal versus input signal level and loop filter response versus loop parameters. The second step concerns the simulation of Telecommand demodulation. This step is composed of Costas loop Telecommand demodulation, clock synchronization and lock indication.

4-1 Simulation of a single main loop PLL

The single main loop PLL of the coherent transponder was tested according to ESA standard, and it has the following parameters:

K_{VCO} = 1000 Hz/V, K_{PD} = 0.5 V/rad, ω_n = 1150 rad/sec, η = 0.8, $2B_{L3dB}$ = 800 Hz and loop filter transfer function is $F(s) = (1.39*10^{-3} s + 1) / (2.37*10^{-3} s)$.

This simulation consists of giving an RF input signal of frequency 9.375 MHz and trying to see the locking behavior between input signal and VCO output signal of frequency 18.75MHz. The circuit diagram for this simulated case is shown in **Fig.(9a)**.

The time domain waveforms for the test points labeled A, B, C, D, E and F are plotted in **Fig.(9b)**.

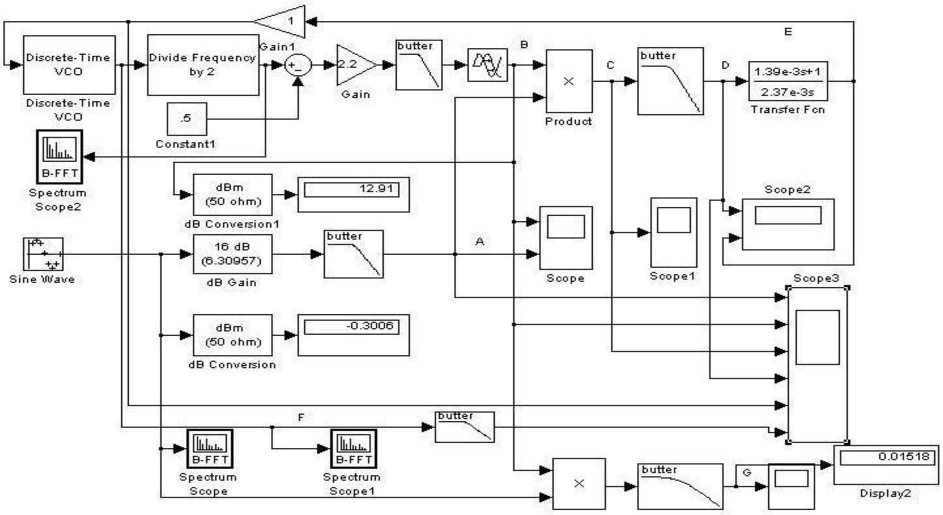

Figure (9a) Single main loop PLL circuit diagram without Doppler shift

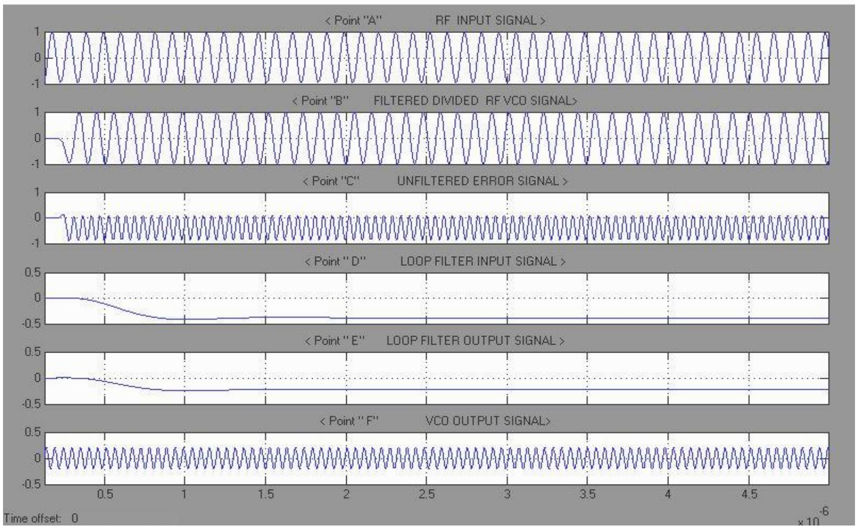

Figure (9b) Time waveforms for single main loop PLL without Doppler shift

The test point labeled A shows an RF input signal of sinusoidal wave at frequency 9.375 MHz with level of ±1 V. Test point B shows a filtered divided VCO signal at frequency 9.375 MHz with level of ±1 V. The error signal at test point C shows a transient behavior during the time (0-250) nsec. The unfiltered error signal reaches after 250 nsec to the steady state with a value of -1 volt. This case indicates that there is very near locking action between the input signal and VCO output signal.

The test point at D shows the input signal to the loop filter defined by F(s). During the period (0–1.8) µsec, there is a transient behavior. After the time 1.8µsec, steady state value is reached with a level of -0.4 volt. Test point E represents the output signal from loop filter. In addition, there is a transient action during (0–1.3) µ sec. There is a steady state value of -0.25 volt during the time (1.3-32) µ sec. Point F shows the output waveform of the VCO. This shows a sinusoidal varying signal of frequency 18.75 MHz with level of ±0.2 V.

4-2 VCO Control Voltage upon Damping Factor Variations

In this simulation, different damping factors (η = 0.2, η = 0.5 and η = 1) are tested to show their effects upon the shape and the value of the VCO control signal (loop filter output signal). The constraint put for this simulation is to fix the 3dB loop bandwidth to 400 Hz according to ESA standard. **Figure (10)** shows the loop filter output signal versus different damping factors.

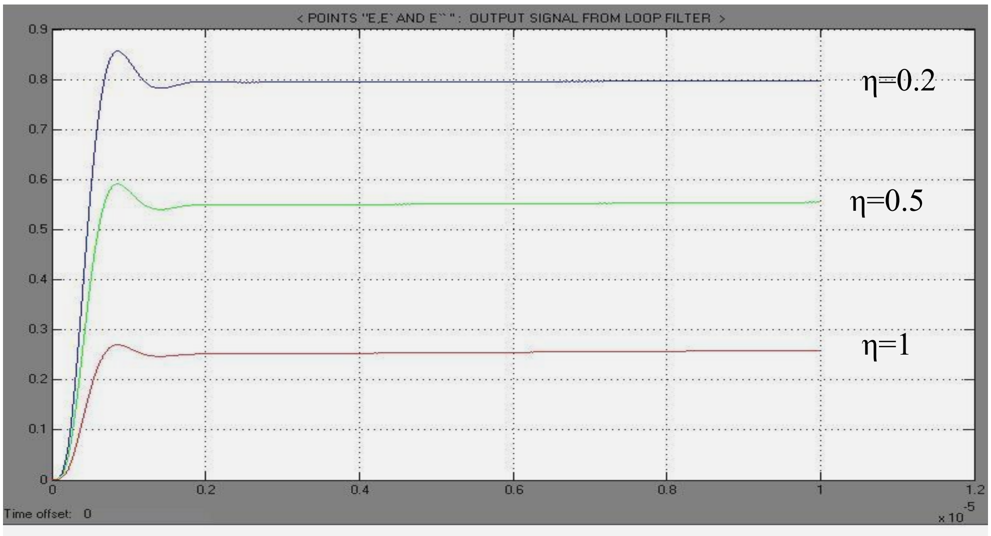

Figure (10) Loop filter output signal versus different damping factors

It is clear from **Fig.(10)** that the output control signal is inversely proportional with the damping factor. In addition, it is noted from **Fig.(10)** that the steady state condition is achieved all in the same time range despite the value of damping factor. The steady state time is (2 – 10) μsec.

4-3 Phase Detector Characteristics

This simulation consists of making a phase difference in steps of 30° starting from 0° to 360° and trying to read the output signal level (tuning VCO signal) under steady state condition. **Table (3)** summarizes the results.

Table (3) VCO control signal versus phase difference

$\Delta\,\Phi$ (degree)	V_{dc} (volt)	$\Delta\,\Phi$ (degree)	V_{dc} (volt)
0	0.5	210	- 0.4308
30	0.4308	240	- 0.247
60	0.247	270	0
90	0	300	0.247
120	- 0.247	330	0.4308
150	- 4308	360	0.5
180	- 0.5		

Plotting the steady state dc value in the table above against the phase difference over the whole 360º, we get **Fig.(11)** which shows the error signal amplitude versus the phase difference.

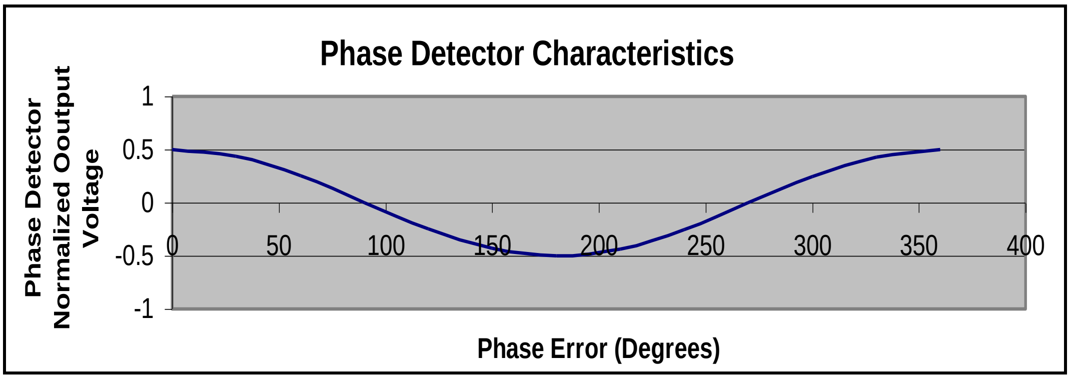

Figure (11) Error signal amplitude versus the phase difference

It is clear from **Fig.(11)** that, when the phase difference is 90º and 270º, the error signal amplitude is zero. The amplitude is maximum at phase difference of 0º and 360º. The response is not linear and has a sinusoidal shape.

4-4 Simulation of Telecommand Detection and Clock Synchronization

The following subsections describe the steps for simulating the space link functions.

I. Costas Loop and Lock Indication Simulation

Costas loop was simulated and tested with the given parameters as:

- Second order type II PLL with $\eta = 0.8$ and $\omega_n = 800$ rad/sec.
- Sensitivity of the VCO block is selected to be 1000 Hz/V.
- Loop filter transfer function is $F(s) = (1 + s\tau_2) / s\tau_1$.

Consider the Costas loop and lock indication circuit model shown in **Fig.(12)**.

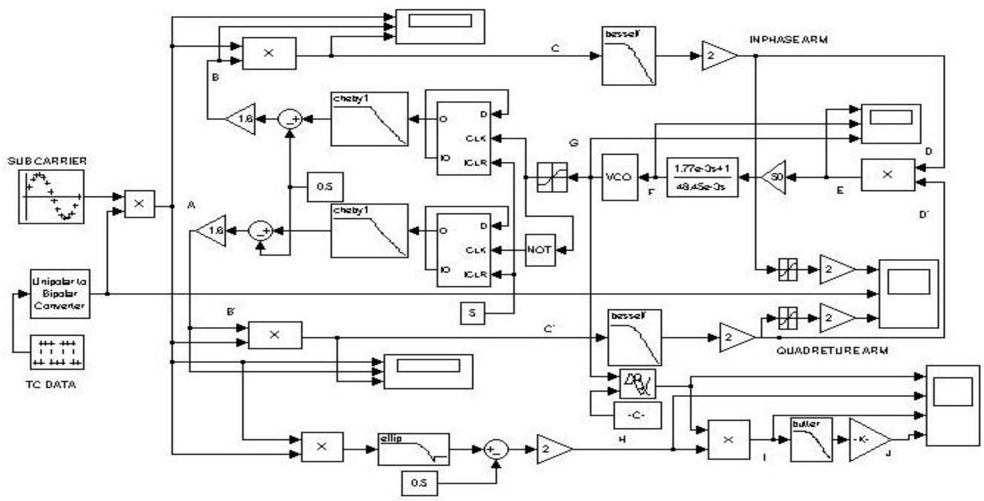

Figure (12) Circuit diagram for Costas recovery loop and subcarrier lock indication

The whole simulation of the Costas recovery loop and lock detection block can be demonstrated through the test point taken as shown in **Fig.(13)**.

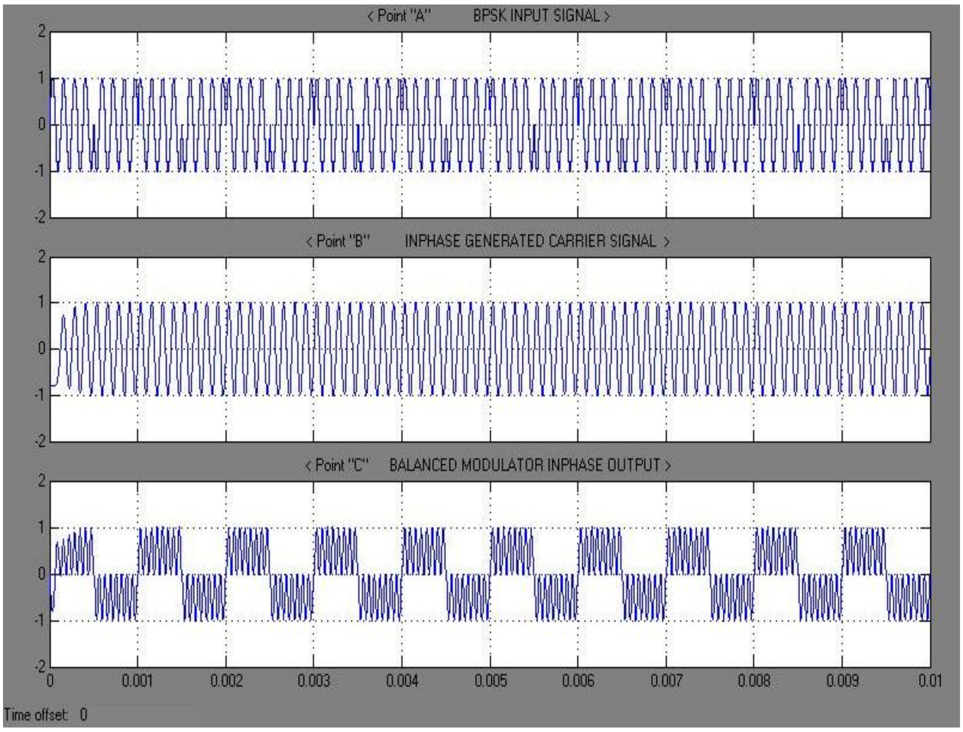

Figure (13a) BPSK input, in phase local carrier and multiplier1 waveforms

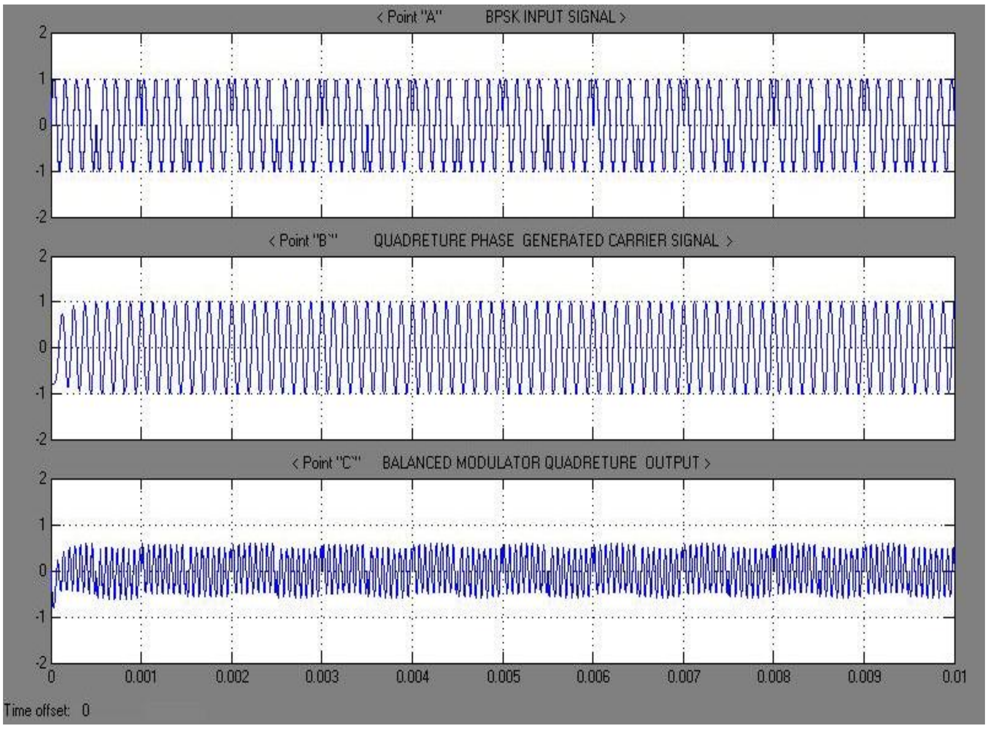

Figure (13b) BPSK input, quadreture phase local carrier and multiplier2 waveforms

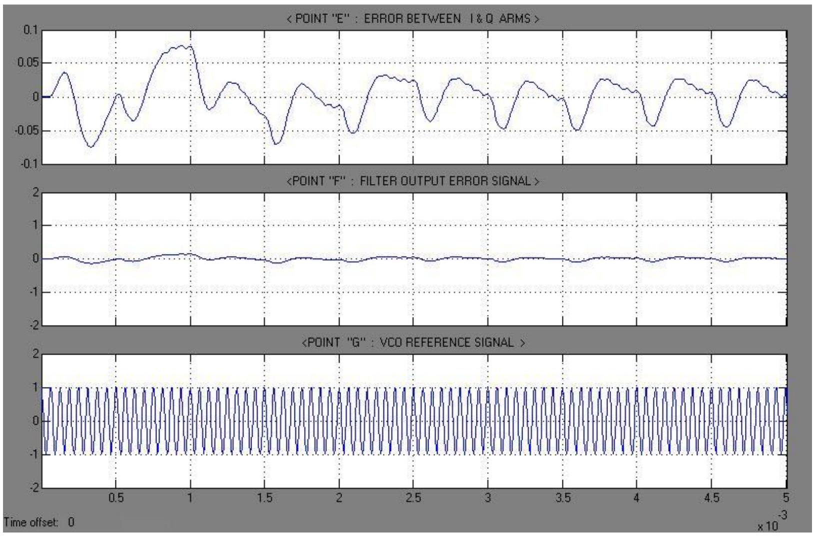

Figure (13c) Error between I&Q arms and VCO reference waveforms

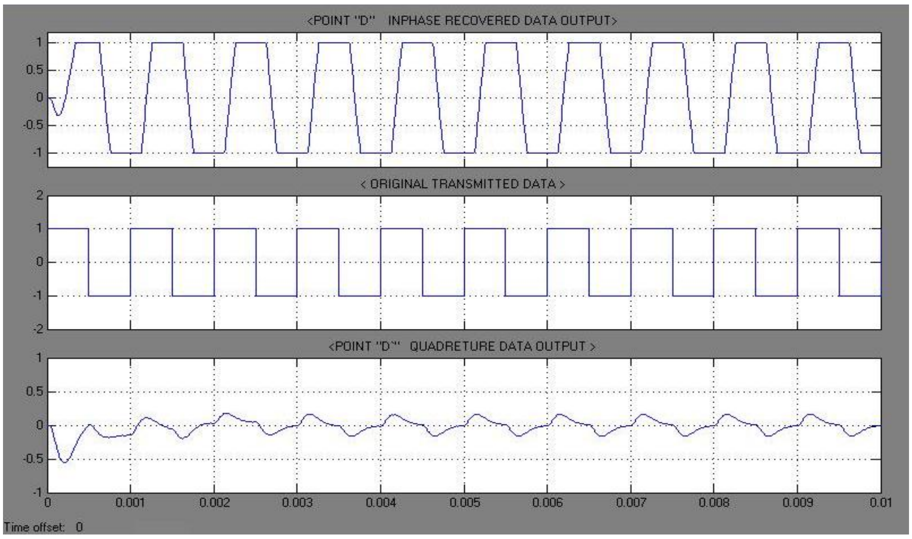

Figure (13d) I&Q arms data output and original TC data waveforms

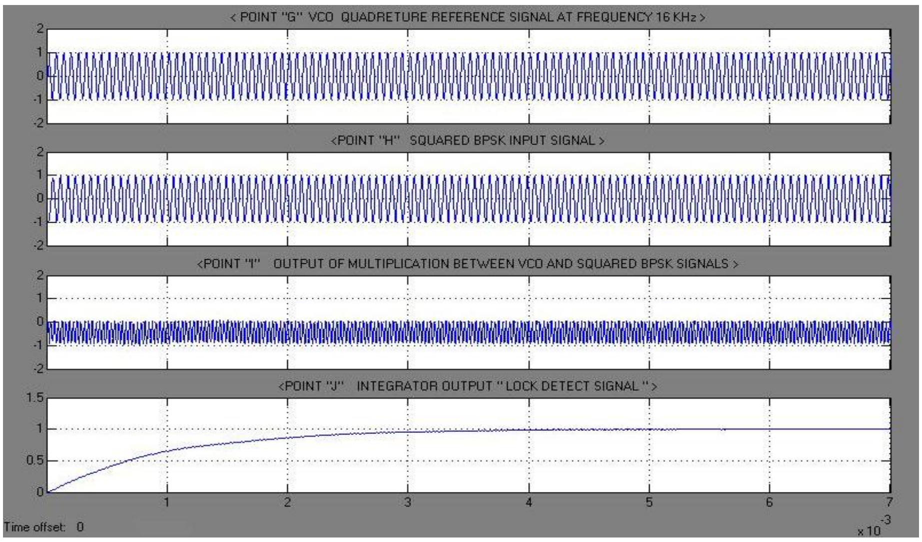

Figure (13e) Waveforms of lock indication procedure

The main point to be considered is the comparison of the recovered data from the inphase data filter arm (point D) and the low pass filter output at the quadreture arm (point D′) with the original transmitted data. From this, it can be said that the signal at point D has a constant envelope and a uniform shape as the original transmitted data. It is clear from figure (13e) that the lock indication block performs logic "1" when the loop operates in right locking conditions. In addition, from the simulation, the lock detect shows a beat note waveform when the VCO is deviated from the nominal frequency.

II. Simulation of Clock Synchronization.

The circuit model for clock synchronization is shown in **Fig.(14a)**. Bit synchronization was simulated with the following given parameters:

- Second order type II PLL with $\eta = 0.8$ and natural frequency f_n is 1% bit rate [15].
- Sensitivity of the VCO block is taken to be 100 Hz/V.
- Loop filter transfer function is $F(s) = (12.7*10^{-3}\ s + 1) / (20*10^{-3}\ s)$.

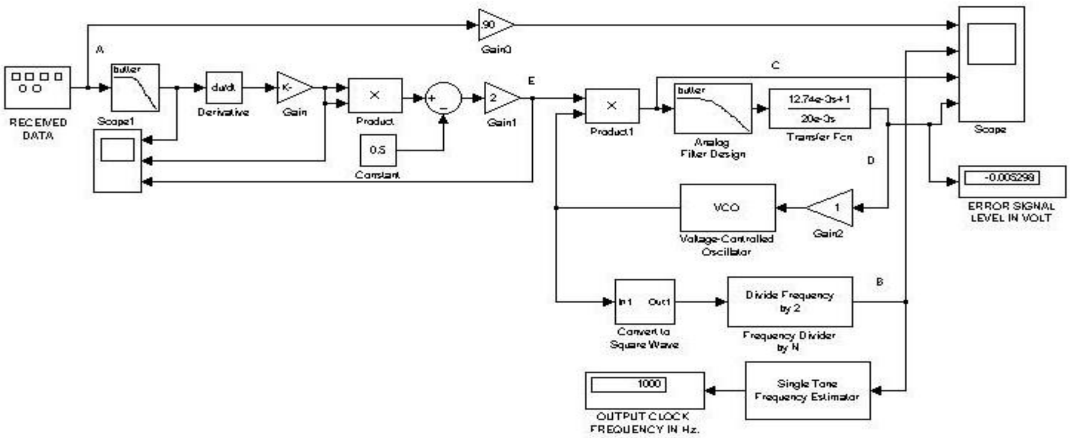

Figure (14a) Circuit diagram for bit synchronization simulation

The overall results for the bit synchronization after simulation are shown in **Fig.(14b)**.

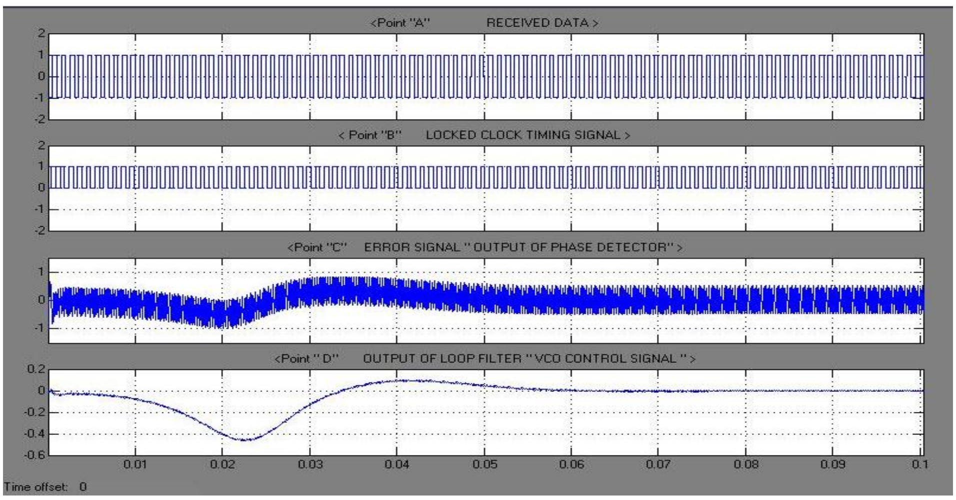

Figure (14b) Timing waveforms for the simulated bit synchronization

It can be noted from **Fig.(14b)** that the waveform shown for test point "B" represents the locked timing clock signal that has a level of 1V and frequency of 1KHz. Test point "C" shows an error signal that is the unfiltered output of the phase detector. Point "D" demonstrates the VCO control waveform that indicates that the loop tracks the input signal.

4-5 Simulation of Main Loop PLL

A main loop PLL unit was simulated with the arrangement shown in **Fig.(15)**.

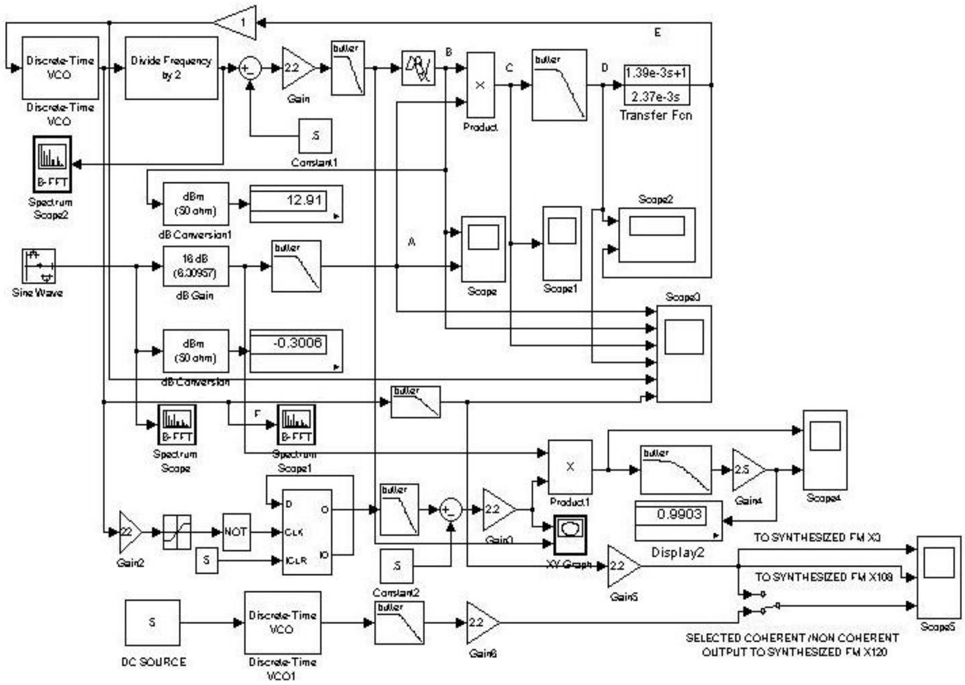

Figure (15) Main Loop PLL unit

The main settings for this simulation can be summarized as follows:

- **DVCO:** Discrete time VCO with power level of 0dBm and sensitivity of 1000 KHz/V. The center frequency for this DVCO is 18.75 MHz.
- **LPF:** Low Pass Filter placed in PLL unit after the phase detector with third order Butterworth response and pass band edge frequency of $6.28*10^6$ rad/sec.
- **Loop Filter:** perfect integrator with $F(s) = (1.39*10^{-3} s + 1) / (2.37*10^{-3}s)$.
- **Input gain block:** suitable gain value of 16dB.
- **Spectrum Scope:** Computes and displays the short-time FFT of each signal.

The input signal for this unit will be taken into two cases:

a. Normal sampled based sinusoidal signal with level of 0.216V. The sampling time is $5.33*10^{-9}$ sec with zero offset samples.

b. Phase modulated BPSK input signal with carrier frequency of 9.375MHz and modulation constant of 0.1rad/V. Subcarrier signal is simulated by time based sinusoidal waveform with level of 5V and frequency of 502.4Krad/sec. The switching TC signal is simulated by a square wave signal with level of 1V and frequency of 10 KHz.

The results of PLL block simulation without modulation can be shown in **Fig.(16)** in terms of the spectra of input, DVCO and divided VCO signals respectively.

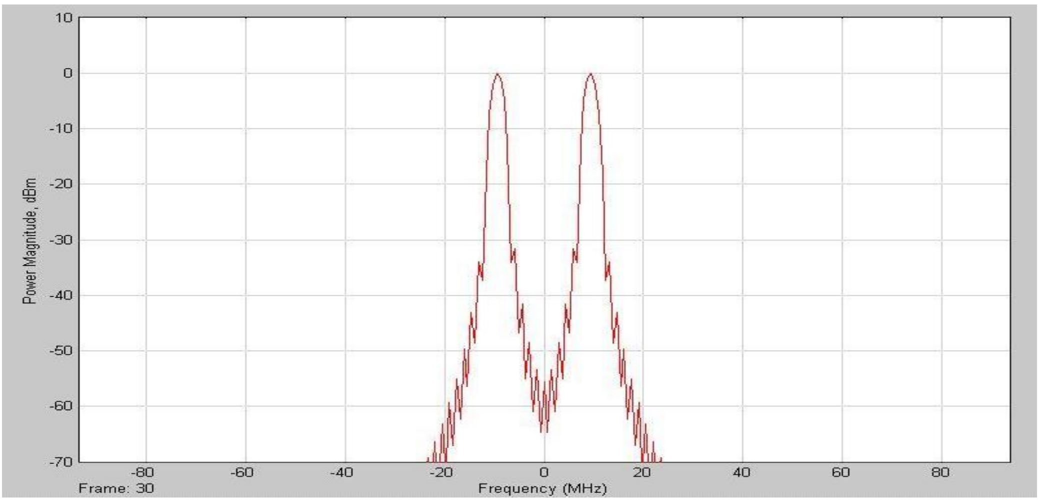

Figure (16a) Spectrum of RF input signal at frequency of 9.375MHz

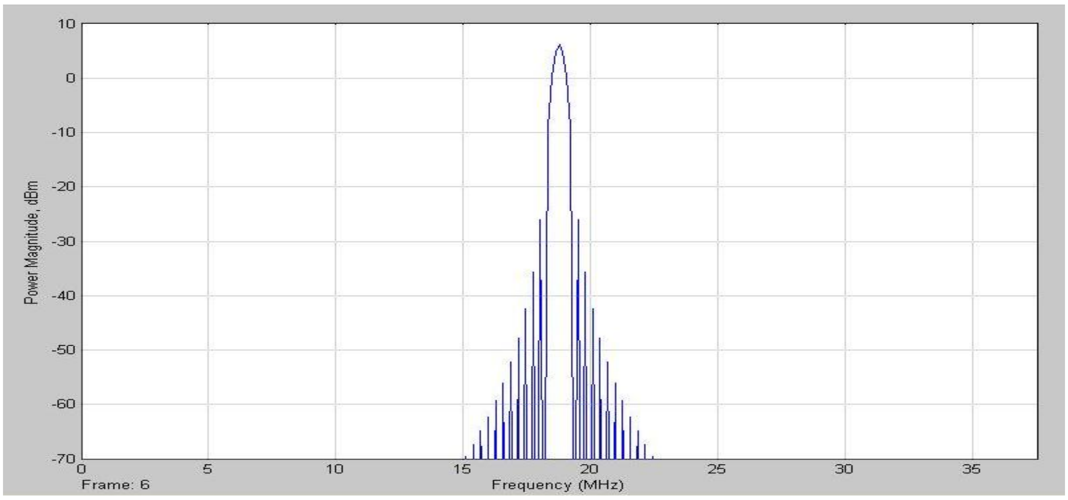

Figure (16b) Spectrum of RF DVCO at frequency of 18.75 MHz

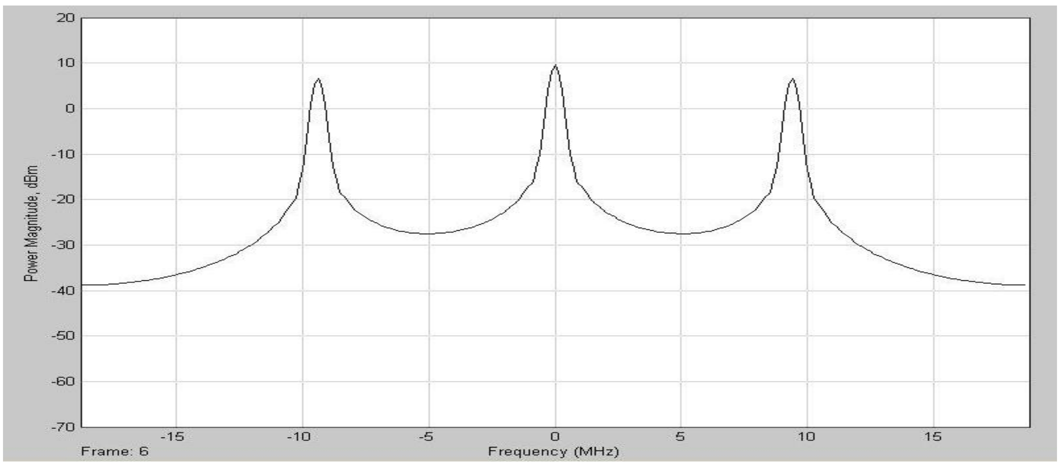

Figure (16c) Spectrum of RF divided DVCO signal at frequency of 9.375MHz

The main loop PLL has to track the input signal and provide lock detect signal when right conditions for locking were achieved. Figure (16d) shows the lock detect waveforms under locking condition.

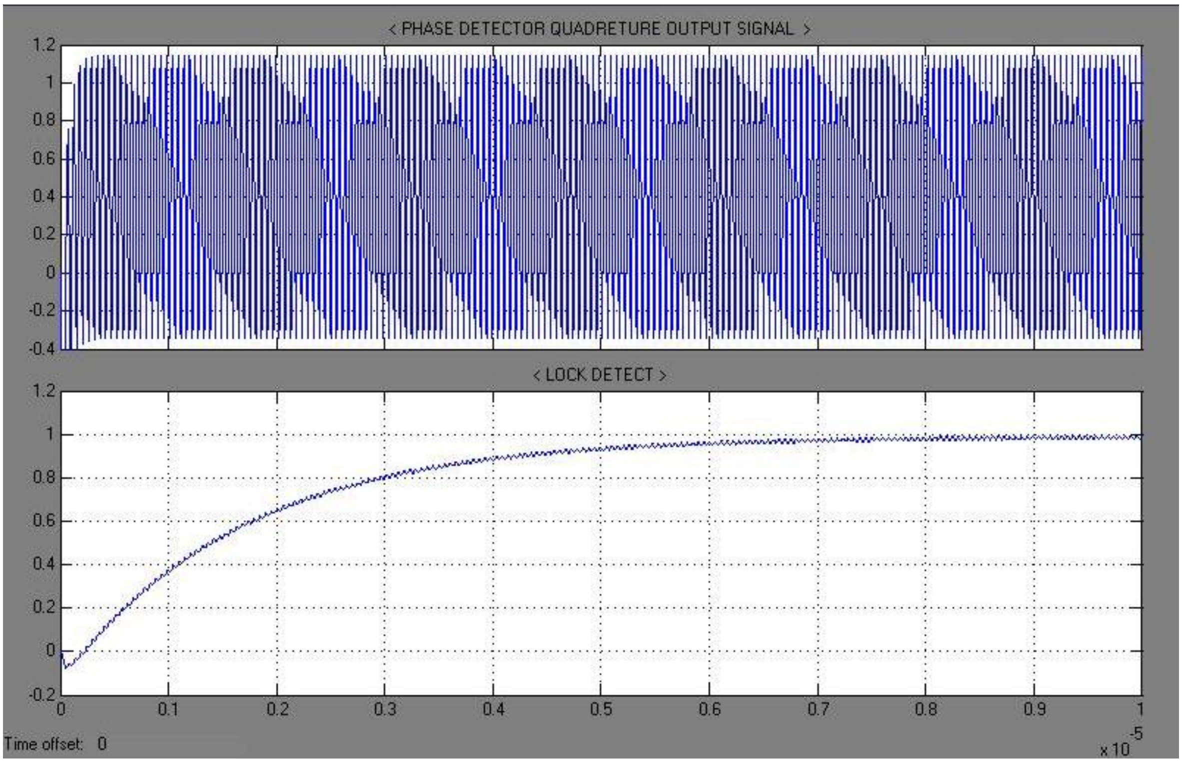

Figure (16d) Lock indication waveform

Under the effect of phase modulation, the simulated circuit diagram is shown in **Fig.(17a)**. The time domain waveforms for this case are shown in **Fig.(17b)**.

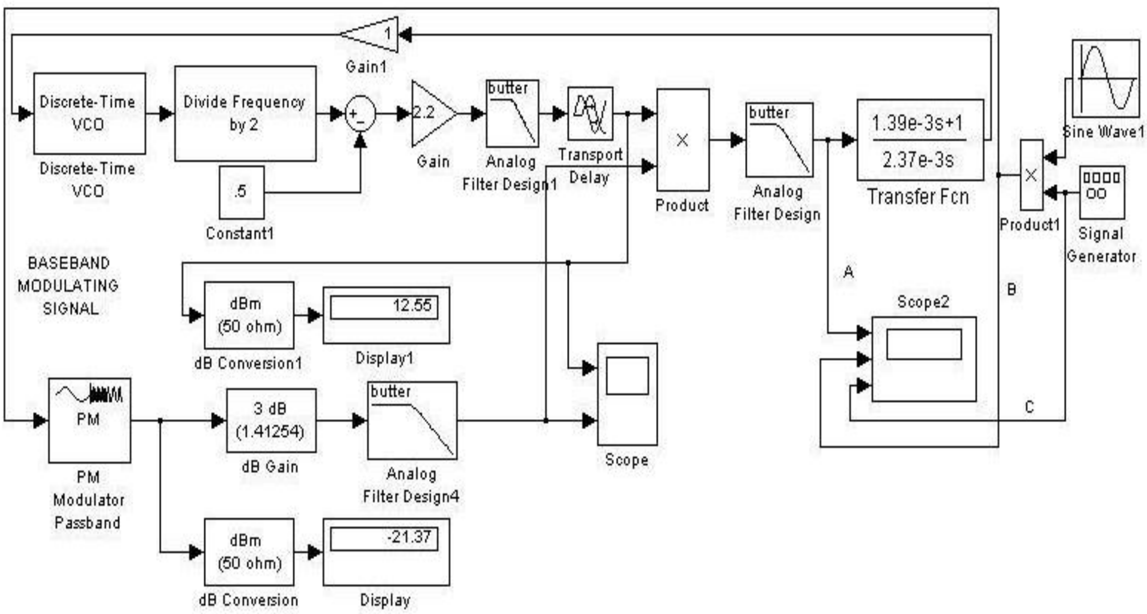

Figure (17a) Main Loop PLL unit under phase modulation

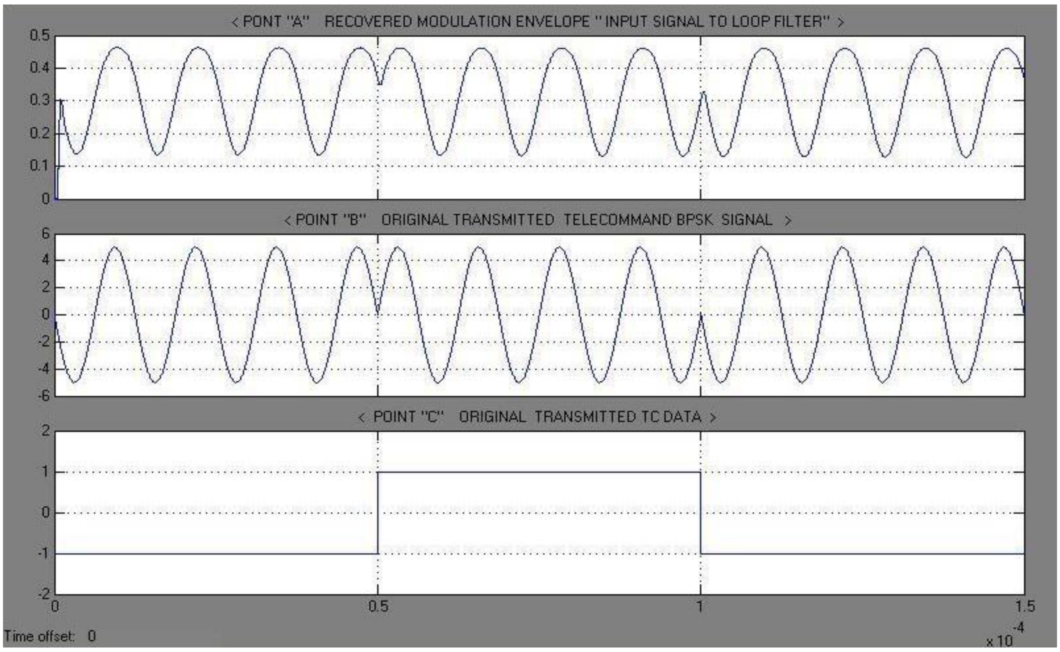

Figure (17b) Phase detector output when BPSK phase modulated RF carrier compared with TC data

5. Conclusions

The coherent transponder is a three loop PLL, which was designed to operate in the frequency range (2025-2120) MHz for uplink (satellite reception) and (2200-2300) MHz for downlink (satellite transmission) with a constraint that is the ratio of downlink to uplink frequency is 240/221.

The following conclusions can be noted:

1. The basic communication functions, i.e., carrier acquisition, TC demodulation, subcarrier lock indication and timing clock synchronization has been performed and tested according to the specification defined by ESA.

2. A basic main loop PLL unit in the coherent transponder has been simulated and tested. The taken test points show a very useful tool for checking the desired response.

3. The engineering model for the coherent transponder as well as the extra functions can be modified to suit the desired specifications, also, to show the effects of parameter variation due to the MATLAB powerful capability before hardware implementation.

4. The value for the damping factor, which was used almost in the entire simulation stages showed to be very reasonable and successful.

5. For single main loop PLL, variation the damping factor affects the value of the VCO control voltage without noticeable effect on the steady state time.

6. The analogue phase detector used in the project has sinusoidal characteristics. Also it is shown that the steady state time does not depend upon the input / output signal under test.

6. References

1. Consultative Committee for Space Data Systems, ***"Recommendations for Space Data System Standards"***, Blue Book, Issue 1&2, May 1999.

2. A., Winton, J., Gerner, P., Michel, and R., Owen, ***"The Transponder-A Key Element in ESA Spacecraft TTC System"***, 2000.

3. M., Marsh, ***"Transponder News"***, 2004.

4. M., Payamifard, H., Hajghassem, and H., Rohi, ***"Design Review of TT&C System in LEO Satellites"***, 2001.

5. E., Vassallo, and R., Madde, ***"ESA's Deep Space and Near Earth Ground Stations for the Next Century"***, 1999.

6. J., C. Freixedas, ***"Spread Spectrum S-Band Transponders for ATV Proximity Link"***, 2nd ESA workshop on Tracking, Telemetry and Command Systems, October 2001.

7. Alcatel Espacio′s News, ***"TTC S-Band Transponder for GOCE Program"***, February 2002.

8. Space Research Center, ***"System Design Document TMTC Subsystem"***, Iraqi Scientific Research Council, 1990.

9. The Standard Approval Board (STAB) for Space Data Communications, ***"Radio Frequency and Modulation Standards"***, ESA PSS-04-105, Issue 1, December 1989.

10. F., Hansen, ***"Spacecraft Telemetry/Telecommand Transponder Design Study"***, Danish Small Satellite Program, 1999.

11. M., Rechharia, ***"Satellite Communication Systems: Design Principles"***, Macmillan Press LTD, 2nd edition, 1999.

12. F. M., Gardner, ***"Phase Lock Techniques"***, John Wiley and Sons. Inc., 2nd Edition, 1980.

13. P. H., Lewis, and W. E., Weingarten, ***"A Comparison of Second, Third and Fourth Order Phase Locked Loop"***, IEEE Trans., AES-3, No.4, July 1967.

14. A., Blanchard, ***"Phase Lock Loop: Application to Coherent Receiver Design"***, John Wiley & Sons, 1978.

15. H. B., Killen, ***"Digital Communication with Fiber Optics and Satellite Applications"***, McGraw-Hill Book Company, 2nd edition, 1988.